Self-Noise and Sensitivity of Broadband Seismographs

A. Gerner & G. Bokelmann

Department of Meteorology and Geophysics (IMGW), University of Vienna

andreas.gerner@univie.ac.at, goetz.bokelmann@univie.ac.at

10TH ANNIVERSARY 15-20|SEPT SALZBURG PANGEO AUSTRIA 2012

universität wien | imgw Institut für Meteorologie und Geophysik

Summary

In this study we investigate self-noise and sensitivity of RefTek™ 151-60A "Observer" broadband seismometers (T_0=60 s, f_0 ≈17 mHz).

We present a self-noise model for this sensor and compare it to the self-noise models of the standard observatory sensor STS-2 (Streckeisen) and RefTek's 151-120 seismometer, which both have natural periods T_0 of 120 s, and are of higher quality and price. We further report on our success of eliminating leakage of the omnipresent microseism noise into self-noise estimates by numerically rotating seismic traces in order to find real self-noise.

Finally, we show that the sensitivity of the 151-60A is sufficient to correctly resolve signals with periods up to approx. ten times its natural period.

Instrument Self-Noise

As improvements of seismic instruments and computational capabilities have promoted the use of increasingly weak seismic signals and seismic noise in seismology, it becomes important to distinguish between the various sources of noise that are recorded in seismic traces (Ringler et al., 2011).

One of these sources of noise is the seismograph itself, which is why for an assessment of its suitability for a given purpose and for reasons of quality control, it is necessary to have a means of estimating the self-noise of an instrument.

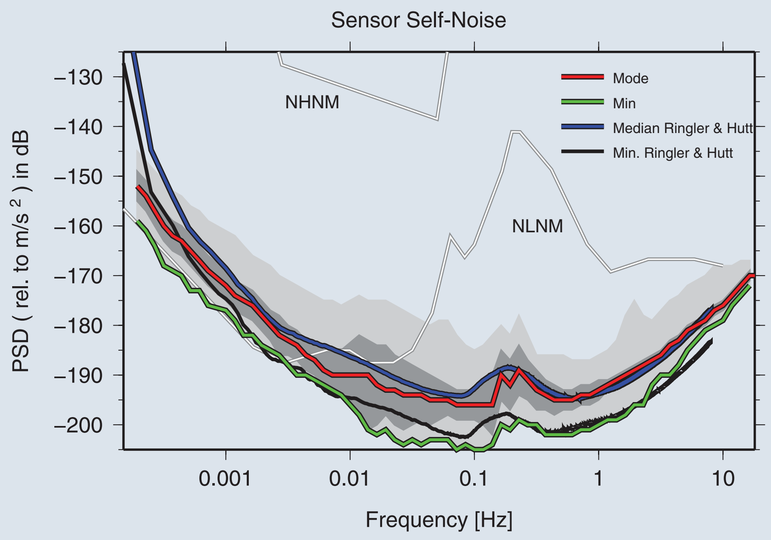

Fig.1: Self-Noise model of the STS-2 as published by Sleeman & Melichar (2012). In all of the self-noise curves the signature of Earth's microseisms, which are the dominant source of natural seismic background noise in the pictured frequency range (Peterson, 1993), can clearly be recognized (also see Ringler & Hutt, 2010).

Sleeman et al. (2006) propose a method of measuring the self-noise of seismographs using coherency analysis. Assuming the seismic background noise recorded by three collocated, co-aligned sensors to be identical, they compute autopower spectra (P_{ii}) and cross-power spectra (P_{ij}) of the recorded data in order to eliminate coherent background noise, and thus isolate and identify the incoherent portion, which can be attributed to the instrument.

Using this technique, for three sensors i,j,k the self-noise of the i^{th} sensor can be expressed as:

$$N_{ii} = P_{ii} - P_{ji} \cdot \frac{P_{ik}}{P_{jk}}.$$

A standardization of self-noise computations based on this method has been proposed by Ringler & Hutt (2010), which would facilitate comparison of different instruments and provide a means to reliably verify a sensor's quality and performance.

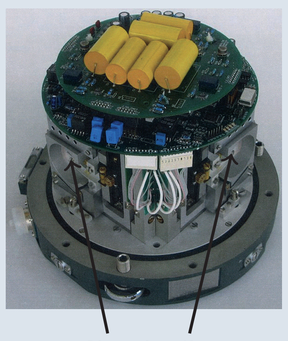

Fig.2: Inside view of a RefTek 151-series broadband sensor.

While intriguingly simple and robust for ideal cases, the self-noise estimates computed with this method strongly depend upon the exact alignment of the collocated instruments. Sleeman & Melichar (2012) show that a misalignment of two stations on the order of 0.2° may cause a significant portion (≈10 dB) of the background noise to leak into the self-noise spectrum. This value of 0.2° is in the range of the max. guaranteeable error in orthogonality of a seismometer's sensing axes. For the 151-60A this error is <0.5° (see Fig.2).

Sensor Alignment and Real Self-Noise

An exact alignment of the horizontal components of three collocated sensors is hard to realize by setup alone. Optimal alignment can subsequently be achieved by numerically rotating the horizontal traces of two sensors about their z-axis, searching for the angles of rotation that minimize their self-noise level in the microseisms band.

We performed a grid-search for best angles of rotation for both horizontal components (ϱ_N & ϱ_E, $\Delta\varrho = 0.02°$). An example is shown in Fig.4. The results for all sensors are listed in Tab.1.

Assuming the horizontal components of all sensors were exactly orthogonal, the angles of rotation ϱ_N & ϱ_E should be identical. Yet, due to limited precision in manufacturing seismometers orthogonality can only be guaranteed within a certain range. For the STS-2 this range is reported to be on the order of 0.2° (Sleeman & Melichar, 2012). Statistically, the standard deviation of our estimates ($\varrho_E - \varrho_N$) from Tab.1 is 0.2°.

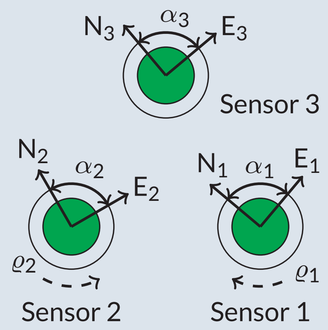

Fig.3: Schematic view of the experiment setup illustrating the misalignment between the three sensors' horizontal components and the rotation performed in this study to align two sensors with the third.

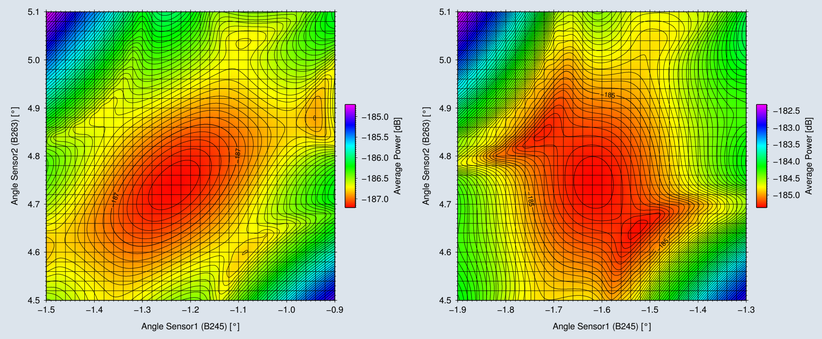

Fig.4: Mean self-noise from numerically rotating two sensors' horizontal components to achieve exact alignment with the third (B267). Left: North/South, Right: East/West.

Sensor 3 ⟹ / Sensor 1/2 ⇓	B209	B220	B221	B224	B225	B226	B234	B245	B263	B267	B32C
B209	0.00	0.30/0.70 **0.40**	-5.31/-5.46 **-0.15**	0.02/0.27 **0.25**	3.27/3.66 **0.39**	0.57/1.03 **0.46**	-0.59/-0.04 **0.55**	2.15/2.83 **0.68**	-3.82/-3.55 **0.27**	0.90/1.23 **0.33**	-0.32/-0.04 **0.28**
B220	-0.30/-0.70 **-0.40**	0.00	-5.61/-6.16 **-0.55**	-0.28/-0.43 **-0.15**	2.97/2.96 **-0.01**	0.27/0.33 **0.06**	-0.89/-0.74 **0.15**	1.85/2.13 **0.28**	-4.12/-4.25 **-0.13**	0.60/0.53 **-0.07**	-0.62/-0.74 **-0.12**
B221	5.31/5.46 **0.15**	5.61/6.16 **0.55**	0.00	5.33/5.73 **0.40**	8.58/9.12 **0.54**	5.90/6.47 **0.57**	4.72/5.42 **0.70**	7.46/8.29 **0.83**	1.49/1.91 **0.42**	6.21/6.69 **0.48**	4.99/5.52 **0.53**
B224	-0.02/-0.27 **-0.25**	0.28/0.43 **0.15**	-5.33/-5.73 **-0.40**	0.00	3.25/3.39 **0.14**	0.55/0.76 **0.21**	-0.63/-0.28 **0.35**	2.13/2.56 **0.43**	-3.84/-3.82 **0.02**	0.88/0.96 **0.08**	-0.34/-0.21 **0.13**
B225	-3.27/-3.66 **-0.39**	-2.97/-2.96 **0.01**	-8.58/-9.12 **-0.54**	-3.25/-3.39 **-0.14**	0.00	-2.68/-2.65 **0.03**	-3.86/-3.70 **0.16**	-1.12/-0.83 **0.29**	-7.09/-7.21 **-0.12**	-2.37/-2.43 **-0.06**	-3.59/-3.60 **-0.01**
B226	-0.57/-1.03 **-0.46**	-0.27/-0.33 **-0.06**	-5.90/-6.47 **-0.57**	-0.55/-0.76 **-0.21**	2.68/2.65 **-0.03**	0.00	-1.18/-1.04 **0.14**	1.57/1.82 **0.25**	-4.40/-4.56 **-0.16**	0.32/0.23 **-0.09**	-0.90/-0.95 **-0.05**
B234	0.59/0.04 **-0.55**	0.89/0.74 **-0.15**	-4.72/-5.42 **-0.70**	0.63/0.28 **-0.35**	3.86/3.70 **-0.16**	1.18/1.04 **-0.14**	0.00	2.75/2.87 **0.12**	-3.23/-3.51 **-0.28**	1.50/1.28 **-0.22**	0.28/0.10 **-0.18**
B245	-2.15/-2.83 **-0.68**	-1.85/-2.13 **-0.28**	-7.46/-8.29 **-0.83**	-2.13/-2.56 **-0.43**	1.12/0.83 **-0.29**	-1.57/-1.82 **-0.25**	-2.75/-2.87 **-0.12**	0.00	-5.97/-6.37 **-0.40**	-1.23/-1.62 **-0.39**	-2.46/-2.77 **-0.31**
B263	3.82/3.55 **-0.27**	4.12/4.25 **0.13**	-1.49/1.91 **-0.42**	3.84/3.82 **-0.02**	7.09/7.21 **0.12**	4.40/4.56 **0.16**	3.23/3.51 **0.28**	5.97/6.37 **0.40**	0.00	4.74/4.75 **0.01**	3.50/3.51 **0.01**
B267	-0.90/-1.23 **-0.33**	-0.60/-0.53 **0.07**	-6.21/-6.69 **-0.48**	-0.88/-0.96 **-0.08**	2.37/2.43 **0.06**	-0.32/-0.23 **0.09**	-1.50/-1.28 **0.22**	1.23/1.62 **0.39**	-4.74/-4.75 **-0.01**	0.00	-1.23/-1.25 **-0.02**
B32C	0.32/0.04 **-0.28**	0.62/0.74 **0.12**	-4.99/-5.52 **-0.53**	0.34/0.21 **-0.13**	3.59/3.60 **0.01**	0.90/0.95 **0.05**	-0.28/-0.10 **0.18**	2.46/2.77 **0.31**	-3.50/-3.51 **-0.01**	1.23/1.25 **0.02**	0.00

Tab.1: Table listing the optimal angles of rotation (ϱ_N/ϱ_E) to align the horizontal components of 11 RefTek 151-60A sensors. Differences of the angles of rotations ($\varrho_E - \varrho_N$) are listed boldfaced below them.

Fig.5: Misalignment of only one single station (B263) primarily manifests itself through leakage of microseism noise into the self-noise estimate of that station (colored lines). This leakage is quite significant, reaching more than 10 dB at 0.3 Hz for 0.5° of misorientation.

Self-noise estimates of the other two stations (not shown here) exhibit only very small variations since they are still well aligned.

If all three stations are misaligned the self-noise estimates become considerably distorted, most significantly in the microseisms band and higher frequencies (dark gray line).

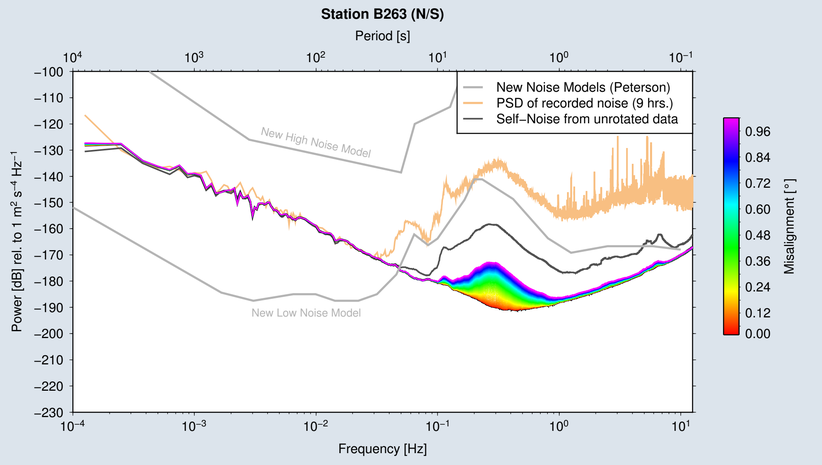

Self-Noise Model for the RefTek 151-60A

Fig.6: Self-noise model for the RefTek 151-60A calculated from data (9 hrs.) recorded at the Conrad Observatory by 15 collocated sensors. Self-noise was computed for all possible permutations of triples of sensors (vertical components only). From the results, 306 self-noise curves of 13 sensors were selected for derivation of this model. To best estimate the true self-noise, curves of clearly misaligned triples of sensors were excluded.

Taking into account the intermediate price of the 151-60A in relation to RefTek's 151-120 or Streckeisen's STS-2, our results compare fairly well with their self-noise models, which have been included in the figure as digitized from the work published by Ringler & Hutt (2010).

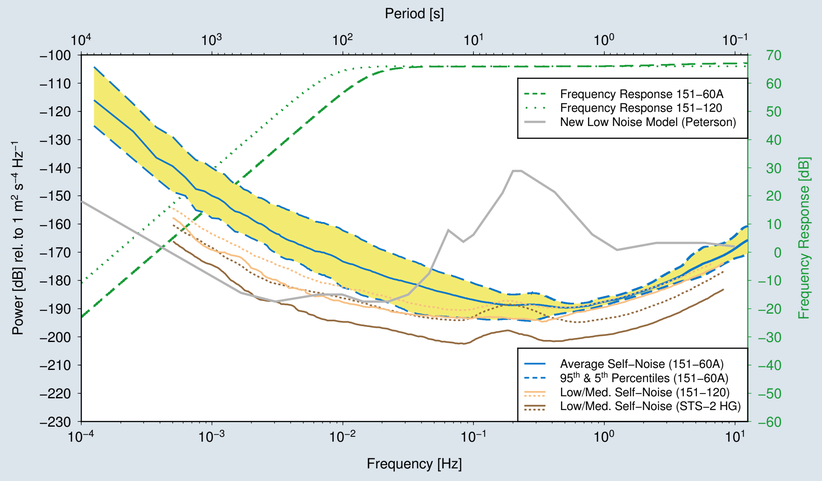

Sensitivity & Earth Normal Modes

Fig.7: Amplitude spectrum of 24 hrs. of data recorded at the Vienna Astronomical Observatory (Sternwarte) by a RefTek 151-60A sensor following the M_W 8.6 Sumatra earthquake from April, 11th 2012 (blue line).

The spectrum is super-imposed on a figure taken from Widmer-Schnidrig & Laske (2007), showing a spectrum of 18 hrs. of data following the M_S 6.7 Australia earthquake (Dec., 12th 2001) recorded at the Black Forest Observatory, Germany (BFO) with Earth's fundamental spheroidal modes ($_0S_l$) labeled in the upper part of the plot.

While stable and in good agreement with the theoretical values of the spheroidal modes up to periods approx. ten times the sensors eigenperiod (1.6 mHz), the calculation of the spectrum tends to become numerically unstable for frequencies below ≈1.4 mHz.

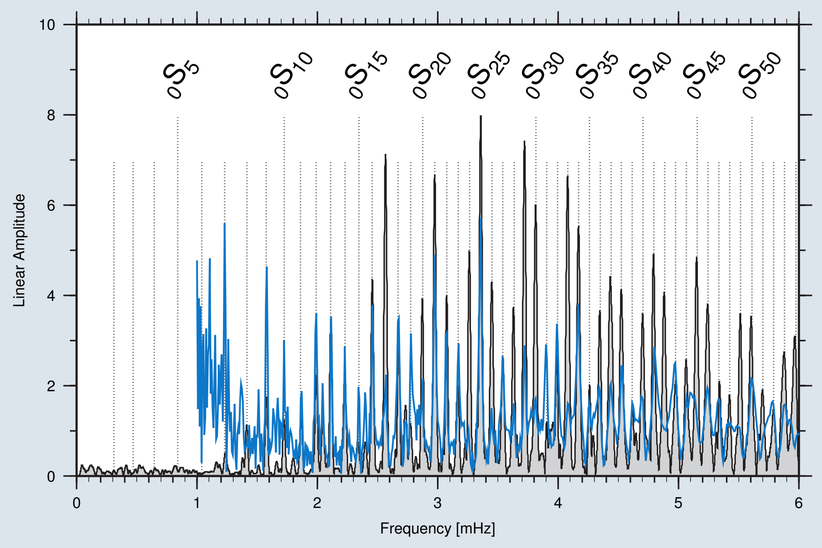

References

Peterson, J., 1993. Observations and Modelling of Seismic Background Noise. In: Open File Report. No. 93-322. U.S. Geological Survey, Albuquerque.

Ringler, A.T., Hutt, C.R., 2010. Self-Noise Models of Seismic Instruments. Seism. Res. Let. 81 (6), 972–983.

Ringler, A.T., Hutt, C.R., Evans, J.R., Sandoval, L.D., 2011. A Comparison of Seismic Instrument Noise Coherence Analysis Techniques. Bull. Seism. Soc. Am. 101 (2), 558–567.

Sleeman, R., Melichar, P., 2012. A PDF Representation of the STS-2 Self-Noise Obtained from One Year of Data Recorded in the Conrad Observatory, Austria. Bull. Seism. Soc. Am. 102 (2), 587–597.

Sleeman, R., van Wettum, A., Trampert, J., 2006. Three-Channel Correlation Analysis: A New Technique to Measure Instrumental Noise of Digitizers and Seismic Sensors. Bull. Seism. Soc. Am. 96 (1), 258–271.

Widmer-Schnidrig, R., Laske, G., 2007. Theory and Observations - Normal Modes and Surface Wave Measurements. In: Treatise on Geophysics. Vol. 1. Elsevier, Cambridge, Ch. 3, pp. 67–125.